

# Generation and characterization of androgen receptor knockout (ARKO) mice: An *in vivo* model for the study of androgen functions in selective tissues

Shuyuan Yeh<sup>\*†</sup>, Meng-Yin Tsai<sup>\*††</sup>, Qingquan Xu<sup>\*</sup>, Xiao-Min Mu<sup>\*</sup>, Henry Lardy<sup>§</sup>, Ko-En Huang<sup>‡</sup>, Hank Lin<sup>\*</sup>, Shauh-Der Yeh<sup>\*</sup>, Saleh Altuwajiri<sup>\*</sup>, Xinchang Zhou<sup>\*</sup>, Lianping Xing<sup>\*</sup>, Brendan F. Boyce<sup>\*</sup>, Mien-Chie Hung<sup>¶</sup>, Su Zhang<sup>¶</sup>, Lin Gan<sup>\*</sup>, and Chawnsang Chang<sup>\*‡||</sup>

<sup>\*</sup>George H. Whipple Lab for Cancer Research, Departments of Urology and Pathology, University of Rochester, Rochester, NY 14642; <sup>§</sup>Institute for Enzyme Research, University of Wisconsin, Madison, WI 53706; <sup>¶</sup>M. D. Anderson Cancer Center, Houston, TX 77030; and <sup>‡</sup>Reproductive Medicine Institute, Chung Gong University, Kaohsiung, Taiwan

Contributed by Henry Lardy, July 29, 2002

**By using a cre-lox conditional knockout strategy, we report here the generation of androgen receptor knockout (ARKO) mice. Phenotype analysis shows that ARKO male mice have a female-like appearance and body weight. Their testes are 80% smaller and serum testosterone concentrations are lower than in wild-type (wt) mice. Spermatogenesis is arrested at pachytene spermatocytes. The number and size of adipocytes are also different between the wt and ARKO mice. Cancellous bone volumes of ARKO male mice are reduced compared with wt littermates. In addition, we found the average number of pups per litter in homologous and heterozygous ARKO female mice is lower than in wt female mice, suggesting potential defects in female fertility and/or ovulation. The cre-lox ARKO mouse provides a much-needed *in vivo* animal model to study androgen functions in the selective androgen target tissues in female or male mice.**

Androgen receptor (AR), a member of the nuclear receptor superfamily, was first cloned in 1988 (1–3). It contains an N-terminal transactivation domain, a central DNA-binding domain, and a C-terminal ligand-binding domain (4). AR may form a dimer and interact with many coregulators to modulate androgen target genes (5). In addition to its natural ligands, testosterone (T) and dihydrotestosterone, 17 $\beta$ -estradiol can also induce AR transactivation in the presence of some selective coregulators in some selective tissues (6, 7). The increasing evidence shows that androgen and AR may also play important roles in female physiological processes, including folliculogenesis (8), bone metabolism (9), autoimmune diseases (10), maintenance of brain functions (11), and several female cancers, including breast, ovary, and endometrium (12–14).

In the cartilage and bone, AR is expressed in chondrocytes, osteoblasts, osteocytes (15), and osteoclasts (16). Clinical studies suggested that combined therapy of estrogens plus androgens may enhance bone mineral density and bone mass to a more significant degree than estrogen therapy alone in postmenopausal women (17, 18). However, the mechanism of androgen action on bone metabolism remains controversial. Some studies suggest that the effect is mainly through the effects of aromatase to transform the androgen to estrogen (19). Other studies show that administration of anti-androgens, including flutamide and casodex, to female mice resulted in osteopenia, suggesting the direct role of AR in bone metabolism (20, 21). As more evidence suggests that estrogens and androgens may have some crosstalk effects, whether estrogen can go through AR, or androgens may go through the estrogen receptor for their physiological functions, remains an interesting question for future studies (22, 23).

Transgenic and knockout (KO) mice have long been used as animal models to study the function of the genes *in vivo*. For AR, the testicular feminization (Tfm) male mice and the patients with the androgen-insensitive syndrome are the natural models for the study of the loss of androgen function in males (24).

However, female models have been lacking, and the classical KO strategy does not work because AR is located in the X chromosome, which is critical for male fertility. To generate tissue-specific ARKO mice or female ARKO mice, a cre-lox strategy for conditional KO is necessary. The cre-lox system utilizes the expression of P1 phage cre recombinase (Cre) to catalyze the excision of DNA located between flanking lox sites (25). This strategy differs from the standard targeted disruption procedure in that embryonic stem (ES) cells are generated in which the targeted segment is not disrupted but flanked by lox sites (floxed). The target gene thus functions normally and mice can be bred to homozygosity for the targeted locus. Here we describe the generation and characterization of ARKO mice. The potential *in vivo* application of this model for the study of androgen functions in selective tissues is also discussed.

## Experimental Procedures

The steps leading to the birth of the female mice carrying the Cre and the homozygous floxed AR genes in both X chromosomes are illustrated in Figs. 1–3. We first constructed the targeting vector followed by generation of the founder mice carrying the floxed AR fragment. The founder mice were then mated with the female Cre mice to generate the F<sub>3</sub> offspring that carries ARKO with Cre expression.

**Construction of Targeting Vectors.** Two genomic clones containing exon 2 of mouse AR were isolated from an ES129/SVJ bacteriophage  $\lambda$  genomic library (Stratagene) by using the mouse AR exon 2 sequence as the probe. The flanking region was sequenced and cloned into the PKI vector (26). Fig. 1 details the procedure for the construction of targeting vectors.

**Generation of the Chimera Founder Mice.** The ES cell line 129/SEVE was grown according to the conditions described (27). For electroporation, 40  $\mu$ g of the targeting vector was linearized by *NotI* and suspended together with 10<sup>9</sup> ES cells in 1 ml of Dulbecco's modified Eagle's medium. They were electropolarized at 300 F, 0.4 ms in the Gene Pulsar II system (Bio-Rad). The neo<sup>r</sup> colonies were selected in the presence of 300  $\mu$ g/ml G418. Homologous recombinations were identified by genomic Southern blot hybridization. The clones with homologous recombination were amplified and reelectropolarized to introduce pCMV-Cre vector into the cells. The transient expression of the Cre in the cells resulted in three types of recombination, which was checked by Southern blot hybridization (27). The ES cells with

Abbreviations: AR, androgen receptor; KO, knockout; ES cell, embryonic stem cell; wt, wild type; T, testosterone; Tfm, testicular feminization; Cre, cre recombinase.

<sup>†</sup>S.Y. and M.-Y.T. contributed equally to this work.

<sup>||</sup>To whom correspondence should be addressed. E-mail: chang@urmc.rochester.edu.

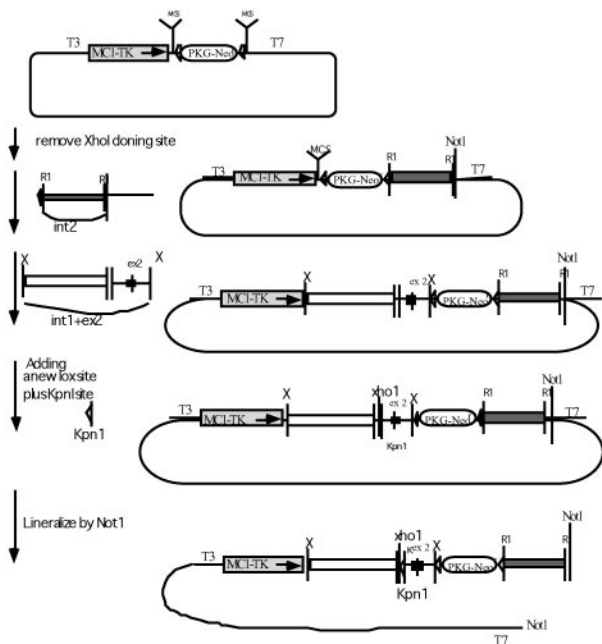


**Fig. 1.** The construction of the floxed AR fragment. The PKI vector is modified from the pBluescript plasmid. It contains a T7 promoter at the 3' end, a T3 promoter at the 5' end, two multiple cloning sites (MCS), two lox sites ( $\blacktriangleright$ ), a positive Neo selective marker (PKG-Neo<sup>+</sup>), and a negative thymidine kinase selective marker (MCT-TK). For the cloning, the *XhoI* site at the 5' end MCS was first destroyed. A 3-kb intron 2 fragment was introduced into the 3' *EcoRI* cloning site (R1), followed by a fragment containing intron 1, exon 2, and a small fragment of intron 2 sequences into 5' *XbaI* site (X). A lox sequence plus an artificial *KpnI* site were finally inserted into the *XhoI* site shortly 5' to the beginning of exon 2. The constructed plasmid was linearized by *NotI* before being electroporated into ES cells.

type 1 recombination were then injected into the inner cell mass of blastocysts, which were then implanted to the uterus of foster mothers for further development.

#### Mating of the Chimera Founder Mice with the Homozygous Cre Mice.

The mating strategy is illustrated (see Fig. 3). The strain of the mosaic founder was C57BL/6J-129/SEVE (B6/129). The mating between the founder and the female B6 mice create agouti female offspring carrying the heterozygous floxed AR (F<sub>1</sub>). The F<sub>1</sub> offspring mate with the B6 male mice to create male mice carrying the floxed AR in the X chromosome (F<sub>2</sub>), or mate with the homozygous ACTB/Cre male that are carrying the Cre under the control of  $\beta$ -actin promoter to generate female mice carrying both the heterozygous floxed AR and Cre (F<sub>2</sub>). Mating these two genotypes of the F<sub>2</sub> mice finally generate female mice carrying the homozygous ARKO and Cre.  $\beta$ -Actin is a house-keeping gene and is universally expressed in every tissue. Therefore, the  $\beta$ -actin promoter-driven Cre will express and delete the floxed AR fragment in all of the cells.

**Primer Design and Genotyping of ARKO Mice.** Based on the sequence information we obtained for the AR genomic DNA, two pairs of primers have been designed to distinguish the wild-type AR (wtAR), ARKO, and floxed AR X chromosome on mice. For examining the ARKO on the X chromosome, the 5' primer named "select" is located in the intron 1 and its sequence is 5'-GTTGATACCTTAACCTCTGC-3', and the 3' end primer is 2-9, which is located in intron 2 and its sequence is 5'-CCTACATGTACTGTGAGAGG-3'. If the mice carry ARKO, the PCR product size from this pair of primers would be 238 bp. If the mouse contains wtAR, this pair of primers will amplify a

PCR product with 580 bp. For examining the floxed AR X chromosome, primer "select" and primer "2-3" are used. 2-3 primer is the 3' end primer which is located in the exon 2 with the sequence 5'-TTCAGCGGCTCTTTTGAAG-3'. This pair of primers will amplify a product with 444 bp. For examining wt AR, the PCR product will be 410 bp. The expression of Cre and internal control IL2 were confirmed by PCR during genotyping. The primer design and PCR conditions of Cre and IL2 follow The Jackson Laboratory's suggestions.

**Histologic Analysis of Bones.** Preparation and analysis of bones were performed, as described (28). In brief, bones were fixed in 10% buffered formalin, decalcified in 10% EDTA, and embedded in paraffin. Sections were stained with hematoxylin and eosin for assessment of bone volume and for tartrate-resistant acid phosphatase activity for quantitation of osteoclasts. Bone volume (amount of bone matrix expressed as a percentage of the cancellous space) and osteoclast numbers (expressed per square millimeter of the cancellous bone volume) in the cancellous space of the long bones were measured. Bone samples were examined from a minimum of four wt and KO mice. Double labeling of bone-forming surfaces was performed by s.c. injection of calcein (20 mg/kg) given 7 days and 1 day before killing. Bone formation rate was measured, as described (29).

**Generation of Osteoclasts.** Splenocytes from ARKO mice and their wt littermates were used to generate osteoclasts in the absence of osteoblast/stromal cells. These cells were incubated with ammonium chloride solution for 10 min on ice to lyse red blood cells, and then cultured ( $1.75 \times 10^5$  cells per well in 96-well plates) in  $\alpha$ -MEM (GIBCO/BRL) supplemented with 10% FCS (HyClone) in the presence of RANKL (100 ng/ml) and M-CSF (10 ng/ml). Cultures were maintained for 5-6 days at 37°C in an atmosphere of 5% CO<sub>2</sub>/air and the media were changed every 2 days by replacing half of the spent media with fresh media supplemented with RANKL/M-CSF. Cells were then fixed and stained for tartrate-resistant acid phosphatase (TRAP) to identify osteoclasts, as described (30).

## Results and Discussion

#### Construction of Targeting Vectors and Electroporation of the ARKO Plasmid in ES Cells.

To disrupt the AR gene, exon 2 is targeted for loxP/Cre-mediated excision. Exon 2 encodes the second zinc finger of the DNA-binding domain, and deletion of the DNA-binding domain has been reported to result in the complete androgen-insensitive syndrome (31). As shown in Fig. 1, the PKI vector was modified from the pBluescript vector and a thymidine kinase-selective marker (MCT-TK) was inserted at the 5' end of the multiple cloning site. The other neomycin-resistant marker (PKG-Neo<sup>+</sup>) flanked by two loxP sequences was inserted at the middle of the multiple cloning site separating it into two parts. The *XhoI*-cloning site was filled in by using Klenow fragment. Two fragments, one was a 3-kb fragment with the intron 2 sequence and the other was a 5-kb fragment including the 3' end of intron 1, exon 2, and the 5' end of intron 2 sequence, were generated by using the extended high fidelity PCR system. The loxP-Cre system utilizes the expression of the P1 phage Cre recombinase to catalyze the excision of DNA located between flanking lox sites. This strategy differs from the standard targeted disruption procedure because the ES cells were generated in which the targeted segment is not disrupted but flanked by lox sites (floxed). The arrangement of loxP sites located in intron 1 and intron 2 can preserve the AR function before Cre introduction. After selection and screening for homologous recombinants, a pCMV-Cre expression plasmid was then transiently transfected into the ES cell clones to induce recombination between any two loxP sites.

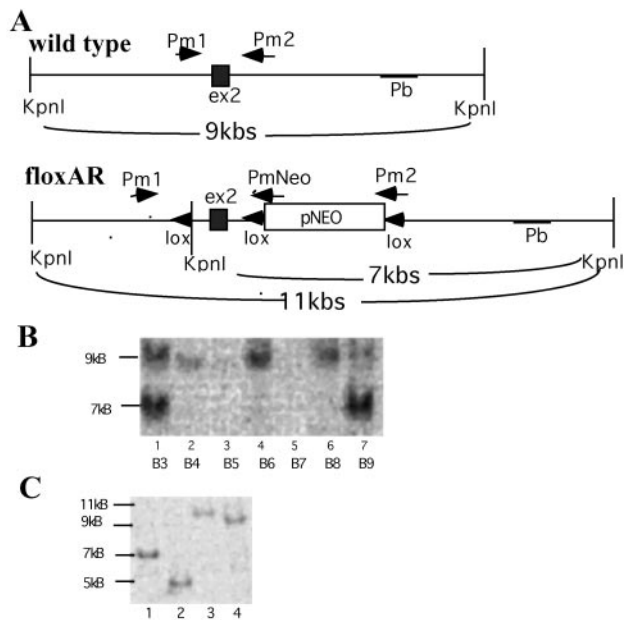


**Fig. 2.** Screening of the extracted DNA to distinguish wtAR from floxed AR. (A) AR fragment and the flanking region. The restriction fragment of *KpnI* in wt is 9 kb. Three lox sites and an artificial *KpnI* restriction site are in the floxed AR fragment. The *KpnI* restriction resulted in one 7-kb and one 4-kb fragment in floxed AR. By using the 3' end sequence as the probe (Pb), the Southern blot hybridization displayed a 9-kb fragment from ES cell clones containing wtAR, and a strong 7-kb fragment from specifically recombined ES cells containing floxed AR plus a weak 9-kb fragment from cocultured STO cells. (B) Southern blot screening of ES cells transfected with floxed AR: B3 and B9 clones are recombined specifically and displayed a strong signal at the 7-kb position from ES cells with floxed AR and a weak signal at the 9-kb position from cocultured STO cells. B4 to B8 are the wt ES clones that displayed signal only at the 9-kb position. (C) Southern blot screening of the floxed AR clone transfected with pCMV plasmid. The pCMV-Cre restricted the sequence between two lox sites and generated four types. Lane 1 is without recombination (7 kb), lane 2 is type I recombination (5 kb), lane 3 is type II (11 kb), and lane 4 is the type III recombination (9 kb).

**Screening of ARKO ES Cells and Genotype Screening of Floxed AR Chimera Male Mice.** For the screening of ES cell clones with ARKO, we designed two pairs of primers to distinguish between the wt and floxed AR locus (Fig. 2A). Southern blotting was applied to verify the floxed AR construct in ES cells (Fig. 2B). The transient transfection of pCMV-Cre would result in type 1, type 2, and type 3 recombinations. As determined by Southern blot analysis illustrated in Fig. 2C, we successfully screened type 1 recombination that represents the floxed AR without Neo. This type 1 recombinant, containing loxP sites flanking the AR exon 2, was then used for the blastocyst injection to generate floxed AR-chimera male mice. With blastocyst injections of two ES clones, A9 and K7, we were able to obtain 6 and 12 floxed AR-chimera male mice, respectively.

**Generation of ARKO Mice.** To generate mice with the disruption of AR, the floxed AR male mice were crossed to female mice carrying Cre under the control of the  $\beta$ -actin (ACTB). ACTB-Cre transcription will be activated in all tissues to generate mice lacking functional AR. As shown in Fig. 3, after two matings, we obtained F<sub>2</sub> mice with male floxed AR mice (floxed AR/Y male) and heterozygous female ARKO on one X chromosome (ar/AR-ACTB/Cre female). We then bred them together to obtain F<sub>3</sub> ARKO female (ar/ar-ACTB/Cre<sup>+/-</sup>) and male (ar/Y-ACTB/Cre<sup>+/-</sup>) mice.

**Genotype Screening of ARKO Mice.** Alternatively, we were able to obtain ARKO male mice by mating floxed AR female and

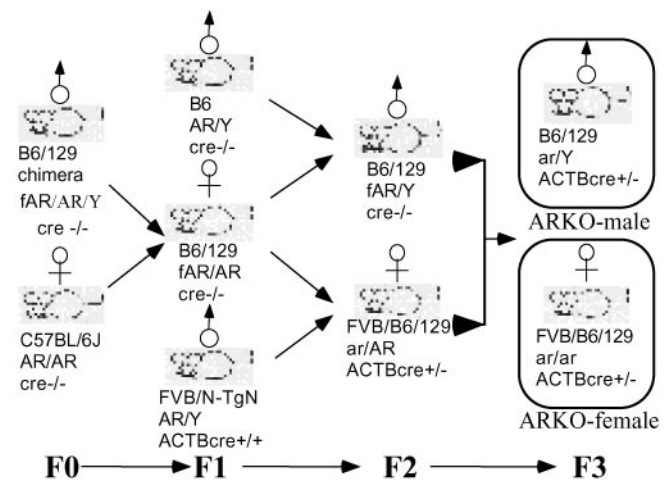


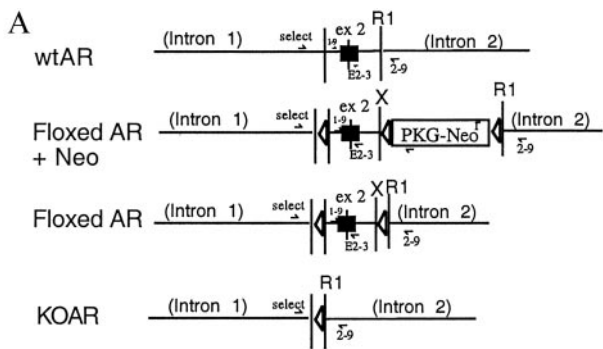
**Fig. 3.** Generation of ARKO female mice by mating among floxed AR founders and cre founders. The chimera founder is B6/129 mosaic strain. The mating of the founder with the B6 female created female mice heterozygous with floxed AR. The following F<sub>2</sub> generation generated floxed AR male mice. The mating between the heterozygous floxed AR female and the homozygous FVB/N-TgN ACTB cre male that carry Cre under  $\beta$ -actin promoter created a heterozygous KO of AR female carrying the Cre. The mating between the floxed AR male and the heterozygous ARKO female carrying the Cre generated the homozygous ARKO Cre<sup>+</sup> female mice with a 1:8 ratio.

ACTB/cre male mice. This strategy will generate pups of four possible genotypes (ar/Y-ACTB/Cre-male, ar/AR-ACTB/Cre-female, AR/Y-ACTB/Cre-male, AR/AR ACTB/Cre-female) with ratio of 1:1:1:1. Three primers, select, exon 2–3, and exon 2–9 (for the relative position of each primer in the AR gene see Fig. 4A), were synthesized to amplify mice genomic DNA to distinguish the floxed AR, ARKO, and wt mice. As shown in Fig. 4, we were able to identify ARKO male mice by using select and exon 2–9 primers to PCR amplify the 238-bp DNA. In contrast, wt mice can produce 580-bp PCR-amplified DNA fragments by using select and 2–9 primers (Fig. 4B).

**Phenotype Characterization of ARKO Male Mice.** Six 5- and 8-week-old ARKO mice were killed for the comparison of their phenotype with wt male and female mice. We first noticed that ARKO male mice have female-like appearance and body weight. In the 5-week-old ARKO male mice, the genito-anal distance is 0.55 cm, similar to female mice, yet is shorter than the wt male mice of 1.05 cm. In the 8-week-old ARKO male mice, the genito-anal distance is 0.59 cm, which is shorter than that of wt male sibling of 1.12 cm and similar to their female siblings (Fig. 5A). The ARKO male mice have testes, yet the size is much smaller, only 20% as compared with the same age of wt male mice (Fig. 5B–D).

**Male Reproductive Organs.** The external genitalia in male ARKO mice showed ambiguous or feminized appearance. The penis seems microphallus and the urethra shows hypospadias. The scrotum is poorly developed and looks like the labia major in the female. All of vas deferens, epididymis, seminal vesicle, and prostate are agenesis (Fig. 5B and C). Testes are small in size and cryptorchid in the low abdominal area close to the internal inguinal ring, and are similar in Tfm mice or humans with complete androgen-insensitive syndrome (Fig. 5B–D). No vaginal opening is found, and also no fallopian tubes and uterus can be observed.

**Analysis of Testes.** To dissect further the testes morphology in the ARKO mice, immunostaining was performed. As shown in Fig.



**B**

Genotype	Primer	PCR size
ACTB Cre+		
-/Y	: select & 2-9	: 238bp
-/X	: select & 2-9	: 238 & 580 bp
X/Y	: select & 2-9	: 580bp
X/X	: select & 2-9	: 580bp

**C**

**Fig. 4.** Genotyping of ARKO mice. We have applied the primers “select” and “2-9” to identify wt and ARKO male mice in our study. (A) Schematic presentation of the DNA construct and primer location in exon 2 area of wt, KO, and floxed AR genes. (B) List of the sizes of PCR product amplified by designed primer pairs. (C) The identification of wt and ARKO mice, by using select and 2-9. We amplified a DNA fragment with 580 bp, which represents wtAR, and with 238 bp, which represents ARKO exon 2. The expression of Cre and internal control IL-2 were confirmed by PCR (Bottom).

6A and B, we could observe obvious AR positive signals in testes from 8-week-old wt mice (Fig. 6A). In contrast, no AR signal could be detected from 8-week-old ARKO mice (Fig. 6B).

We then compared the histology of testes from ARKO mice and wt mice. As shown in Fig. 6C and D, in the testes from wt mice, spermatogenesis sequentially developed round spermatids and elongated spermatids. In addition, mature spermatozoa can be clearly observed (Fig. 6C). However, testes from ARKO mice are less cellular and thin in the seminiferous tubules. Some tubules contain Sertoli cells only and the others contain a few germ cells (Fig. 6D). In the tubules with germ cells, the spermatogonia are hypoplastic. Occasionally, some spermatocytes at the pachytene stage are found (Fig. 6E). No round spermatids, elongated spermatids, or mature spermatozoa occur in the whole testis, suggesting spermatogenesis may be arrested at pachytene

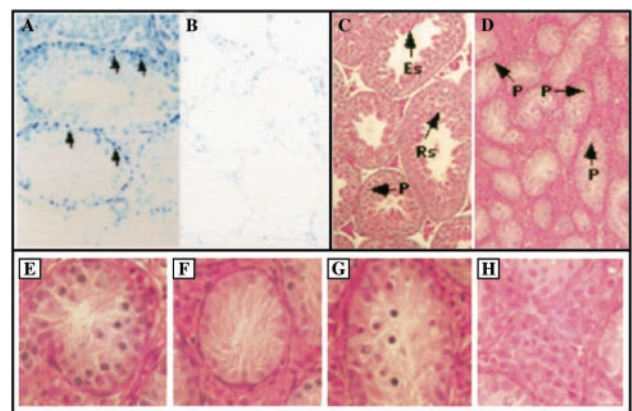


**Fig. 6.** Immunostaining of AR and histologic analysis of testes from wt and ARKO male mice. Immunostaining of AR in testes from wt (A) and ARKO mice (B). For AR staining, anti-AR antibody and Vectorstain ABC-AP kit were used according to the manufacturer's procedures. Testes from wt show positive signal (A, arrows), and testes from ARKO mice show no positive staining. ( $\times 40$ ) The histology of the testis from wt (C) and ARKO (D) shown by hematoxylin and eosin stain. Spermatogenesis in ARKO mice arrested in pachytene spermatocyte (P) stage. ( $\times 40$ ) Rs, round spermatids; Es, elongated spermatids; P, pachytene spermatocytes. In further analysis of testes in complete ARKO mice we obtained the following information (E–H): (E) The tubule contains hypoplastic spermatogonia and pachytene spermatocyte. (F) The tubule contains Sertoli cells only and shows fibrillary degeneration in the cytoplasm of Sertoli cells. (G) Some cells in the tubule contain condensed and pyknotic nuclei. They may represent apoptotic bodies. (H) Leydig cells located in interstitial space are hypertrophic.

spermatocyte. The Sertoli cells show fibrillary degeneration (Fig. 6F). Many pyknotic cells contain apoptotic-like bodies in tubules (Fig. 6G). In the interstitial space, Leydig cells are hypertrophic (Fig. 6H).

Early studies showed that testes in Tfm mice are smaller (20% of normal), cryptorchidic, and composed of immature tubular elements surrounded by several layers of peritubular cells and enlarged Leydig cells. The numbers of Leydig cells are normal or slightly reduced. The reduced seminiferous tubules contain only Sertoli cells, spermatogonia, and primary spermatocytes. Spermatogenesis was arrested at the spermatocyte stages or earlier. In older Tfm mice, the Leydig cells seemed to be hypertrophied. In the pachytene spermatocytes stage, homologues are fully paired and exchange of genetic material occurs through crossing over between chromatids of homologous chromosomes (32). Together, our results indicate AR may play some important roles during these processes.

**Testosterone Concentration in Serum.** Previous *in vivo* animal models clearly established that initiation, maintenance, and reinitiation of spermatogenesis are androgen-dependent processes (33). We also compared the serum T concentration in 8-week-old mice in wt and ARKO mice. The results from three individual mice indicate that the T concentration in ARKO mice is lower than wt mice.

**Bones.** Histologic analysis of bone sections from 8-week-old ARKO mice shows that cancellous bone volumes are lower in the ARKO mice than in both female and male wt littermates. The decrease in bone volume is seen readily in the metaphyses of the femora (Fig. 7A and C) and tibiae (data not shown). Osteoclast numbers in the femoral metaphyses are higher in ARKO than in wt mice (Fig. 7C). However, the number of osteoclasts formed *in vitro* from spleen cells from ARKO mice is similar to that in wt mice (data not shown). Mean values for mineral apposition and bone formation rates in the femoral

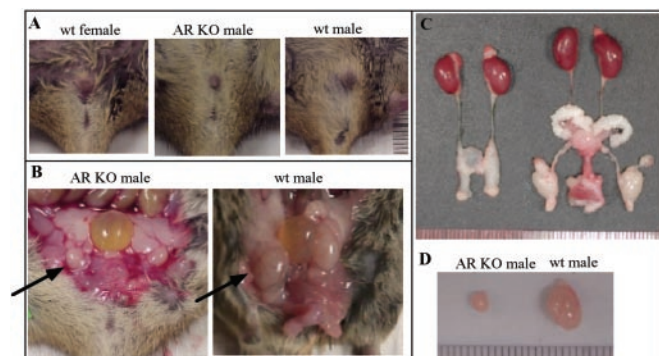


**Fig. 5.** Phenotype of 8-week-old male ARKO mice. Six 8-week-old male ARKO mice were killed. The results were always compared among siblings. (A) The external genitalia of male ARKO, wt male, and wt female. (B and C) The internal genitalia of male ARKO and wt male mice. Arrows in B identify the testis. (D) The testes of wt male and ARKO mice.

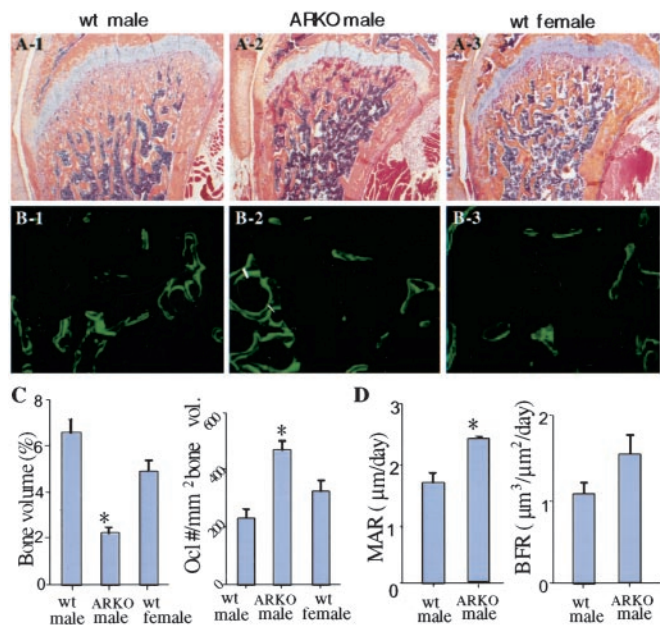


**Fig. 7.** Bone phenotype in ARKO mice. (A) Hematoxylin and eosin-stained femoral bones of 8-week-old wt and ARKO mice. Note the decreased trabecular bone area in the distal metaphysis of the ARKO mouse compared with wt littermates. (B) Calcein double labeling in 8-week-old wt and ARKO mice. The mean distance between the two yellow labels (white lines) represents the rate of bone mineralization from which the rate of bone formation is calculated. (C) Bone volume and osteoclast numbers data in ARKO and wt mice. Data are from six ARKO male mice and the same number of male and female littermates. (D) Mineral apposition and bone formation rate data in ARKO and wt mice. Data are from three ARKO mice and the same number of wt littermates. \*, statistically significant differences compared with control mice ( $P < 0.05$ ). Error bars represent SD.

metaphyses are higher in the ARKO mice (Fig. 7B and D) than in the wt mice. The difference in the values for bone formation rates did not reach statistical significance, presumably because of the small number of animals studied (three per group). These data indicate that in the absence of the AR, mice develop osteopenia. Because osteoclast numbers and bone formation are both increased in these mice, the osteopenic phenotype most likely is because of bone resorption being increased beyond that of the increase in bone formation. This increase in osteoclast function could be the result of an imbalance in the production of RANKL (the major osteoclastogenic cytokine) and OPG (the major inhibitor of RANKL, which inhibits RANKL by acting as its decoy receptor) by osteoblast/stromal cells (34), because estrogen regulates OPG production by these cells (35). We have demonstrated previously that testosterone and estrogen promote apoptosis of osteoclasts and their precursors *in vitro* and *in vivo* (34, 36). Thus, it is possible that osteoclasts are not only increased in number in ARKO mice, but that they also live longer than normal because of reduced testosterone concentrations, and therefore resorb more bone than wt cells. These possibilities are currently under investigation. The increased bone mineral apposition and bone formation rates coupled with increased osteoclast numbers and low bone volumes observed in the mice is a phenotype that is seen in sex steroid deficiency (37) and is consistent with the low T concentrations in the mice. Taken together, the osteopenic phenotype of ARKO mice strongly supports an important role of AR signaling in bone metabolism.

**Body Weight and Adipose Tissue.** The body weight of ARKO male mice is similar to wt female mice with an average of 18.8 g at 5

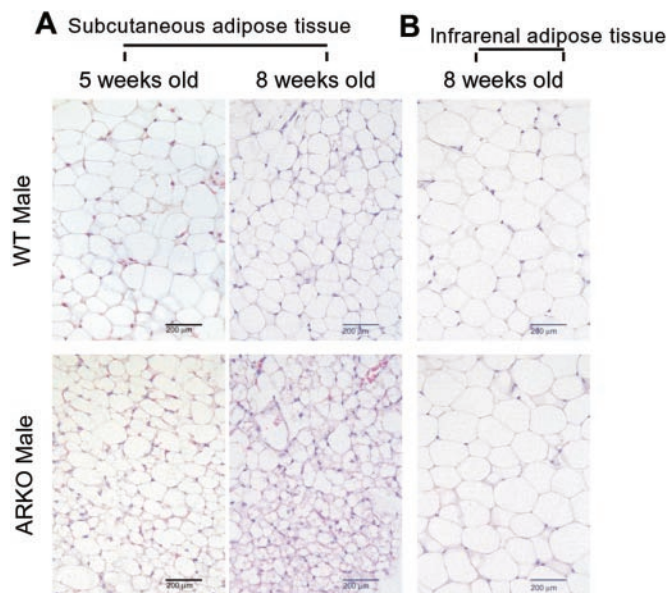


**Fig. 8.** Histology of fat tissues in ARKO mice. (A) s.c. adipose tissue of 5- and 8-week-old ARKO and wt littermates were stained with hematoxylin and eosin. (Bars = 200 μm.) (B) Infrarenal adipose tissue of 8-week-old ARKO and wt littermates were stained with hematoxylin and eosin. (Bars = 200 μm.)

weeks and 20.1 g at 8 weeks. In contrast, the average body weight of wt male mice is 24.3 g at 5 weeks and 26.7 g at 8 weeks. Histologic analysis of adipose tissue indicated that the size and number of adipocytes start to be different between wt male and ARKO male mice at 5 weeks. These differences become more obvious in 8-week-old mice (Fig. 8A). In contrast, infrarenal adipocytes were well-developed in both 5- and 8-week-old mice, and show no obvious difference between wt and ARKO mice (Fig. 8B). These results suggest that AR may play roles in adipogenesis. Early reports also suggest that androgens may play some roles in the site specificity of adipose metabolism (38). Women with abdominal fat distribution may have increased percentage of free T in the peripheral blood. In contrast, obesity in men may be characterized by reduced T. However, the detailed mechanisms of how T-AR influence adipose tissue and obesity remain unclear. Because peroxisome-proliferator-activated receptors play important roles in adipogenesis (39, 40) and the AR coregulator, ARA70, can modulate both AR and peroxisome-proliferator-activated receptors' transcriptional activities (41, 42), it will be interesting to see whether AR can crosstalk to peroxisome-proliferator-activated receptors' pathway by sharing a common coregulator, such as ARA70, in adipose tissue.

**ARKO Female Mice.** Because of the infertility of Tfm male mice, it is difficult to generate ARKO female mice to study the roles of AR in female tissues. With floxed AR male mice, we now are able to mate them with ACTB-Cre ar/AR-female to generate ARKO in female mice. By using this strategy, we were able to obtain a few ARKO female mice, and we are in the process of obtaining more ARKO female mice and analyzing their phenotypes with focus on the ovary and breast.

Early analysis showed that although the female ARKO were fertile, the average number of the pups per litter from heterozygous and homologous ARKO females are reduced as compared to wt female mice. Even though we obtained homologous ARKO female mice, we are still in the process of obtaining enough mice for further analysis. Previous studies have revealed that androgens played a positive role in the early stage of folliculogenesis

(43, 44). However, it is unclear whether the androgen effect is mediated by AR. For example, Vendola *et al.* suggested that this effect could be mediated by way of growth factor signal pathways instead of the AR-mediated pathway (44). With ARKO female mice, we are in the process of dissecting potential roles of AR in the folliculogenesis.

The morphology of breast in our ARKO mice at this early stage show no major differences as compared with wt mice. Early studies suggested that androgen-AR may play some roles in the progression of breast cancer (45). The detailed mechanisms, however, remain unclear. Our ARKO female mice may provide a nice *in vivo* model to study how carcinogens induce breast tumors in the presence versus absence of AR in breast tissue.

**Tissue-Specific Knockout of AR.** One advantage of creating the floxed AR mice is to provide a base to generate tissue-specific ARKO in selective tissues such as breast (mating with MMTV-Cre mice), prostate (mating with PSA-Cre or probasin-Cre), and liver (mating with  $\alpha$ -fetal protein-Cre or albumin-Cre). We are in the process of generating these tissue-specific ARKO mice to study the roles of AR in these tissues.

In summary, the generation of ARKO male and female mice provides us with a valuable *in vivo* model to study androgen functions in selective tissues.

This work was supported by National Institutes of Health Grants DK60905 and AR43510, U.S. Army Grant DAMD17-02-1-0557, and the George H. Whipple Professorship Endowment.

- Chang, C. S., Kokontis, J. & Liao, S. T. (1988) *Science* **240**, 324–326.
- Chang, C. S., Kokontis, J. & Liao, S. T. (1988) *Proc. Natl. Acad. Sci. USA* **85**, 7211–7215.
- Lubahn, D. B., Joseph, D. R., Sullivan, P. M., Willard, H. F., French, F. & Wilson, E. M. (1988) *Science* **240**, 327–330.
- Chang, C., Saltzman, A., Yeh, S., Young, W., Keller, E., Lee, H. J., Wang, C. & Mizokami, A. (1995) *Crit. Rev. Eukaryotic Gene Expression* **5**, 97–125.
- Heinlein, C. A. & Chang C. (2002) *Endocr. Rev.* **23**, 175–200.
- Yeh, S., Miyamoto, H., Shima, H. & Chang, C. (1998) *Proc. Natl. Acad. Sci. USA* **95**, 5527–5532.
- Zhou, Z. X., He, B., Hall, S. H., Wilson, E. M. & French, F. S. (2002) *Mol. Endocrinol.* **16**, 287–300.
- Donath, J., Michna, H. & Nishino, Y. (1997) *J. Steroid Biochem. Mol. Biol.* **62**, 107–118.
- Compston, J. E. (2001) *Physiol. Rev.* **81**, 419–447.
- Olsen, N. & Kovacs, W. J. (2001) *Immunol. Res.* **23**, 281–288.
- Poletti, A. & Martini, L. (1999) *J. Steroid Biochem. Mol. Biol.* **69**, 117–122.
- Liao, D. J. & Dickson, R. B. (2002) *J. Steroid Biochem. Mol. Biol.* **80**, 175–189.
- Wang, P. H., Chao, H. T., Liu, R. S., Cho, Y. H., Ng, H. T. & Yuan, C. C. (2001) *Gynecol. Oncol.* **83**, 596–598.
- Sasaki, M., Dahiya, R., Fujimoto, S., Ishikawa, M. & Oshimura M. (2000) *Mol. Carcinog.* **27**, 237–244.
- Benz, D. J., Haussler, M. R., Thomas, M. A., Speelman, B. & Komm, B. S. (1991) *Endocrinology* **128**, 2723–2730.
- Mizuno, Y., Hosoi, T., Inoue, S., Ikegami, A., Kaneki, M., Akedo, Y., Nakamura, T., Ouchi, Y., Chang, C. & Orimo, H. (1994) *Calcif. Tissue Int.* **54**, 325–326.
- Davis, S. R., McCloud, P., Strauss, B. J. & Burger, H. (1995) *Maturitas* **21**, 227–236.
- Castelo-Branco, C., Vicente, J. J., Figueras, F., Sanjuan, A. & Martinez de Osaba, M. J. (2000) *Maturitas* **34**, 161–168.
- Schweikert, H. U., Rulf, W., Niederle, N., Schafer, H. E. Keck, E. & Kruck, F. (1980) *Acta Endocrinol.* **95**, 258–264.
- Weisman, Y., Cassorla, F., Malozowski, S., Krieg, R. J., Jr., Goldray, D., Kaye, A. M. & Somjen, D. (1993) *Steroids* **58**, 126–133.
- Lea, C. K. & Flanagan, A. M. (1999) *J. Endocrinol.* **160**, 111–117.
- Migliaccio, A., Castoria, G., Di Domenico, M., de Falco, A., Bilancio, A., Lombardi, M., Barone, M. V., Ametrano, D., Zannini, M. S., Abbondanza, C. & Auricchio, F. (2000) *EMBO J.* **19**, 5406–5417.
- Panet-Raymond, V., Gottlieb, B., Beitel, L. K., Pinsky, L. & Trifiro, M. A. (2000) *Mol. Cell. Endocrinol.* **167**, 139–150.
- Soule, S. G., Conway, G., Prelevic, G. M., Prentice, M., Ginsburg, J. & Jacobs, H. S. (1995) *Clin. Endocrinol. (Oxford)* **43**, 671–675.
- Holt, C. L. & May, G. S. (1993) *Gene* **133**, 95–97.
- Wang, S. W., Kim, B. S., Ding, K., Wang, H., Sun, D., Johnson, R. L., Klein, W. H. & Gan, L. (2001) *Genes Dev.* **15**, 24–29.
- Kaczmarczyk, S. J. & Green, J. E. (2001) *Nucleic Acids Res.* **29**, E56–E66.
- Xing, L., Venegas, A. M., Chen, A., Garrett-Beal, L., Boyce, B. F., Varmus, H. E. & Schwartzberg, P. L. (2001) *Genes Dev.* **15**, 241–253.
- Ducy, P., Desbois, C., Boyce, B., Pinero, G., Story, B., Dunstan, C., Smith, E., Bonadio, J., Goldstein, S., Gundberg, C., Bradley, A. & Karsenty, G. (1996) *Nature* **382**, 448–452.
- Xing, L., Bushnell, T. P., Carlson, L., Tai, Z., Tondravi, M., Siebenlist, U., Young, F. & Boyce, B. F. (2002) *J. Bone Miner. Res.* **17**, 1200–1210.
- He, W. W., Kumar, M. V. & Tindall, D. J. (1991) *Nucleic Acids Res.* **19**, 2373–2378.
- Vornberger, W., Prins, G., Musto, N. A. & Suarez-Quian, C. A. (1994) *Endocrinology* **134**, 2307–2316.
- Roberts, K. P. & Zirkin, B. R. (1991) *Ann. N.Y. Acad. Sci.* **637**, 90–106.
- Suda, T., Takahashi, N., Udagawa, N., Jimi, E., Gillespie, M. T. & Martin T. J. (1999) *Endocr. Rev.* **20**, 345–357.
- Saika, M., Inoue, D., Kido, S. & Matsumoto, T. (2001) *Endocrinology* **142**, 2205–2212.
- Hughes, D. E., Dai, A., Tiffée, J. C., Li, H. H., Mundy, G. R. & Boyce, B. F. (1996) *Nat. Med.* **2**, 1132–1136.
- Hughes, D. E., Jilka, R., Manolagas, S., Dallas, S. L., Bonewald, L. F., Mundy, G. R. & Boyce, B. F. (1995) *J. Bone Miner. Res.* **10**, S150.
- Dieudonne, M. N., Pecquery, R., Boumediene, A., Leneuve, M. C. & Giudicelli, Y. (1998) *Am. J. Physiol. Cell Physiol.* **274**, C1645–C1652.
- Brun, R. P., Kim, J. B., Hu, E., Altiok, S. & Spiegelman, B. M. (1996) *Curr. Opin. Cell Biol.* **8**, 826–832.
- Chawla, A., Schwarz, E. J., Dimaculangan, D. D. & Lazar, M. A. (1994) *Endocrinology* **135**, 798–800.
- Yeh, S. & Chang, C. (1996) *Proc. Natl. Acad. Sci. USA* **93**, 5517–5521.
- Heinlein, C. A., Ting, H. J., Yeh, S. & Chang, C. (1999) *J. Biol. Chem.* **274**, 16147–16152.
- Weil, S., Vendola, K., Zhou, J. & Bondy, C. A. (1999) *J. Clin. Endocrinol. Metab.* **84**, 2951–2956.
- Vendola, K., Zhou, J., Wang, J., Famuyiwa, O. A., Bievre, M. & Bondy, C. A. (1999) *Biol. Reprod.* **61**, 353–357.
- Bentel, J. M., Birrell, S. N., Pickering, M. A., Holds, D. J., Horsfall, D. J. & Tilley, W. D. (1999) *Mol. Cell. Endocrinol.* **154**, 11–20.